A major purpose of the Technical Information Center is to provide the broadest dissemination possible of information contained in DOE's Research and Development Reports to business, industry, the academic community, and federal, state and local governments.

Although a small portion of this report is not reproducible, it is being made available to expedite the availability of information on the research discussed herein.

LA-UR-84-138
CONF-8310169-2

NOTICE
PORTIONS OF THIS REPORT ARE ILLEGIBLE.
It has been reproduced from the best available copy to permit the broadest possible availability.

Los Alamos National Laboratory is operated by the University of California for the United States Department of Energy under contract W-7405-ENG-36

LA-UR--84-138

DE84 006014

TITLE: ANALYSIS OF ANELASTIC RELAXATIONS CONTROLLED BY A SPECTRUM OF RELAXATION TIMES

AUTHOR(S): J. R. Cost

SUBMITTED TO: Proceedings of Symposium, "Nontraditional Methods in Diffusion," Philadelphia, Penn., October 4 & 5, 1983

DISCLAIMER

Los Alamos Los Alamos National Laboratory
Los Alamos, New Mexico 87545

ANALYSIS OF ANELASTIC RELAXATIONS CONTROLLED BY A SPECTRUM OF RELAXATION TIMES

J. R. Cost

Los Alamos National Laboratory
Los Alamos, New Mexico 87545
USA

Summary

Anelastic studies, although they have provided an important method for investigating the mobility of point defects in solids, have often been difficult to analyze when a continuous spectra of relaxation times controls the anelastic response. This paper describes a new method for obtaining accurate estimates of relaxation time spectra by direct analysis (without prior assumptions) of the data using a nonlinear regression method. Applications to internal friction and anelastic creep results are described with emphasis upon the internal friction technique.

Introduction

Studies of relaxation processes by anelastic methods provide an important method for investigating the mobility of atomic defects and solutes in crystalline solids. Two main kinds of anelastic experiments are used to study relaxation phenomena, internal friction referred to as dynamic measurements and anelastic creep or quasi-static measurements. The many investigations using these methods cover a wide range of materials, species of defects and kinds of relaxations. For an excellent review covering the breadth of this area the reader is referred to the book by Nowick and Berry (1).

One of the main goals in both internal friction and anelastic creep measurements is to determine the relaxation time, τ. This time can often be associated with some average jump time of a point defect or solute atom. Knowledge of this time then provides information about the atomic mobility or diffusivity of the relaxing entity. For example, with the Snoek relaxation, which is the stress-induced motion of interstitial solutes in body-centered cubic metals, the diffusivity can be obtained directly from the relaxation time τ by the relation $D = a^2/(36\tau)$, where a is the lattice parameter. Simple well-behaved relaxation processes such as the Snoek relaxation may be characterized by a single relaxation time. If this is the case, the value of τ is easily obtained for either the internal friction or the anelastic creep measurements. For the former it is obtained from the relation $\omega\tau = 1$ which applies for the maximum in the internal friction peak with ω being the angular frequency of the experiment. For the anelastic creep measurements, the creep follows simple exponential decay so that τ is obtained simply as the time constant for decay.

The above analyses become considerably more complicated when the relaxation process involves either multiple relaxations or a spectrum of relaxation times instead of a single time. It then becomes necessary either to determine each of several discrete relaxation times when the number of discrete relaxations is unknown or to determine the spectral density for what may be a relatively complicated distribution of relaxation times. The purpose of this paper is to present a new method for direct analysis of relaxation data which yields a close approximation of the actual spectrum of relaxation times. This method is unlike conventional methods because it directly analyzes the data without making prior assumptions concerning the form of the spectrum. Conventional methods, on the other hand, usually assume various spectra and then choose the best one based upon goodness-of-fit to the data.

This new method has previously been presented and validated for a wide variety of relaxation time spectra applied to the first-order kinetics of anelastic creep (2, 3). The main thrust of this paper will be to apply and validate the same method for internal friction results. With the availability of this method, future internal friction measurements may then be directly analyzed to obtain the appropriate relaxation time spectrum and thus help to avoid the controversies which tend to develop because data have been force-fit to assumed spectra. This capability has already been used to resolve a long-standing controversy concerning the analysis of anelastic creep measurements (4).

Computer analysis of anelastic results has already been used extensively; however, the method described here and in Ref. (1) is the first to directly yield the relaxation time spectrum. A possible reason why direct analysis methods have not been developed in the past is because it was felt that such methods would only be useful for data which had unattainably high accuracy. An important part of this development of the method is assessment of its applicability to data with various amounts of experimental error. Interestingly, it will be shown that the method is not highly sensitive to the magnitude of the random error. Instead, subtle differences in the overall shape of an anelastic response curve are most important for the analysis.

Background

For a discussion of the problems which develop when a spectrum of relaxation times is involved instead of a discrete relaxation time, it is first necessary to briefly describe the experimental methods and the relationships which govern the anelastic response. This will be done for two main anelastic methods, internal friction which describes the dynamic response and anelastic creep which describes the quasi-static behavior. These descriptions will necessarily be abbreviated, and the reader is again recommended to the definitive treatment by Nowick and Berry (1). Their terminology and symbols have been used through most of this chapter. In order to discuss the internal friction and anelastic creep behavior it is necessary to make use of a simple model, the standard anelastic solid, to fully describe anelastic behavior in its most elemental form.

Standard Anelastic Solid

The standard anelastic solid is a two-spring, single-dashpot model in which one spring is in parallel and the other is in series with the dashpot. The dashpot has a time constant τ which determines the time-dependent or anelastic behavior of the model. As it will be used here, τ is the relaxation time at constant stress, referred to as τ_σ by Nowick and Berry.

For a standard anelastic solid upon application of a constant stress σ at $t = 0$, the dashpot resists extension of the spring in parallel and the spring in series extends elastically to strain ϵ_{el} so that the unrelaxed compliance is $J_u = \epsilon_{el}/\sigma$. Similarly, at $t \gg \tau$ the dashpot is fully extended so that the anelastic or time-dependent strain ϵ_{an} has occurred and the compliance is the relaxed compliance $J_r = (\epsilon_{el} + \epsilon_{an})/\sigma$. The difference $J_r - J_u = \delta J$, which is the compliance of just the parallel dashpot and spring part of the model, is a measure of the strength of the anelastic relaxation. Thus the standard anelastic solid is a 3-parameter model which can be fully described by J_u, δJ and τ for both internal friction and anelastic creep behavior.

Internal Friction

For dynamic experiments the stress is applied periodically at frequency ω so that for an anelastic system there will be phase lag of the strain behind the stress. The angle of this phase lag is ϕ, the loss angle and the compliance is described by two dynamic response functions, a real part $J_1(\omega)$ and an imaginary part $J_2(\omega)$. The internal friction is given by

$$\tan \phi(\omega) = J_2(\omega)/J_1(\omega) \tag{1}$$

For the standard anelastic solid model responding to a periodic stress, the two dynamic response functions are given by

$$J_1(\omega) = J_u + \frac{\delta J}{1 + (\omega\tau)^2} \tag{2}$$

$$J_2(\omega) = \delta J \frac{\omega\tau}{1 + (\omega\tau)^2} \tag{3}$$

which are the equations derived by Debye to describe dielectric relaxation as a function of frequency ω. These two equations, which are for a single relaxation time, will later be modified so that they apply to a spectrum of relaxation times. It should be noted that Eq. (3) describes the familiar internal friction peak which has a maximum at $\omega\tau = 1$. Also, if $J_2(\omega)$ for a standard anelastic solid is plotted as log $\omega\tau$, the curve is symmetrical about log $\omega\tau = 1$.

The above description is for measurements at constant τ of tan ϕ (ω) as a function of frequency; however, internal friction is more conveniently measured as a function of temperature at constant (or nearly constant) frequency. This is possible since the relaxation time can usually be assumed to obey the Arrhenius relation,

$$\tau = \tau_0 e^{Q/kT} \tag{4}$$

where T is absolute temperatures, τ_0 is a pre-exponential factor, Q is the activation energy, and k is Boltzmann's constant. Eq. (4) may be substituted into Eqs. (1)-(3) to give an expression for the internal friction as a function of temperature. For this case the internal friction is plotted versus 1/T so that a Debye peak will still be symmetrical about its maximum. Such a plot will scale according to the previously-discussed plot versus log ω but with scale factor $Q/2.3k$ since

$$\log(\omega\tau) = \log(\omega\tau_0) + (Q/2.3k)\ (1/T) \tag{5}$$

The reader is referred to Ref. (1) which discusses in detail the corrections that are required due to problems such as variations of ω, δJ and J_u with temperature. Because of the importance of the measurement of internal friction versus temperature (as opposed to frequency) the final goal of the analysis described in this paper will apply to that case. However, the analysis method which is to be described for treating internal friction controlled by a spectrum of relaxation times is equally applicable to the isothermal measurements described by Eqs. (1)-(3). Since this method avoids the corrections required with varying temperature, it will be used in most of the portions which follow. Thus, it may be considered that the subsequent plots of internal friction versus log ω can equally be considered as plots versus 1/T, but with an appropriate scale factor $Q/2.3k$ as given by Eq. (5).

Anelastic Creep

The quasi-static behavior of a standard anelastic solid will be described for the experimental condition of measuring strain versus time at constant stress. (The analogous experiments of measuring stress at constant strain yields a similar treatment but will not be discussed.) Thus, as with the internal friction measurements the subscript σ indicating constant stress will be assummed. i.e., $\tau = \tau_\sigma$. The strain measurements to be described are all at constant temperature and are made with $t = 0$ the time at which a new state of stress σ is applied after equilibration for a time $t_{eq} \gg \tau$ at a prior stress. Typically the experiments measure either anelastic creep following an equilibration at zero stress or the recovery of this anelastic creep following removal of the equilibration stress. In either case for a standard anelastic solid the fractional change in the anelastic strain $\epsilon(t)$ is given by

$$\Psi(t) = \frac{\epsilon_0 - \epsilon(t)}{\epsilon_0 - \epsilon_\infty} = 1 - \exp(-t/\tau) \tag{6}$$

where ϵ_0 and ϵ_∞ are the initial and final (equilibrium) strains. Eq.(6) indicates that the normalized anelastic creep obeys simple first-order kinetics for both the load-on and the load-off experiments described above. Since only a single relaxation time controls the response, the value of τ is obtained directly from the time constant for this decay.

Relaxation-Time Spectra

We now consider how the internal friction and anelastic creep behavior as described in the previous section are affected when a distribution of relaxation times replaces the single time constant. Consider $N(\ell n\ \tau)$ a distribution function for a spectrum (on a logarithmic scale) of relaxation times which governs the anelastic response. Here τ is taken as a ratio to some reference value and thus is unitless. Also, $N(\ell n\ \tau)$ is normalized to unity such that

$$\int_{-\infty}^{\infty} N(\ell n\ \tau)\, d\, \ell n\ \tau = 1 \tag{7}$$

This and subsequent integrations are over $\ell n\ \tau$ rather than τ following normal practice for presenting relaxation time spectra.

Applying this normalized relaxation time spectrum to the real and imaginary compliances which define the internal friction we obtain

$$J_1(\omega) = J_u + \delta J \int_{-\infty}^{\infty} N(\ell n\ \tau)\, \frac{1}{1+(\omega\tau)^2}\, d\, \ell n\ \tau \tag{8}$$

$$J_2(\omega) = \delta J \int_{-\infty}^{\infty} N(\ell n\ \tau)\, \frac{\omega\tau}{1+(\omega\tau)^2}\, d\, \ell n\ \tau \tag{9}$$

Thus the internal friction $\tan \phi = J_2/J_1$ has an integral in both the numerator and the denominator. If the magnitude of the anelastic effect is small, i.e., if $\delta J \ll J_u$, as is often true, then $J_1 \simeq J_u$ so that we can eliminate the integral in the denominator and from Eqs. (1) and (8) obtain

$$\tan \phi(\omega) \simeq \Delta \int_{-\infty}^{\infty} N(\ell n\tau)\, \frac{\omega\tau}{1+(\omega\tau)^2}\, d\, \ell n\ \tau \tag{10}$$

Here we use the substitution

$$\Delta = \delta J/J_u \tag{10a}$$

where Δ is referred to as the relaxation strength. Applying the same method as was used to obtain Eqs. (8) and (9) we obtain for the fractional anelastic creep

$$\Psi(t) = 1 - \int_{-\infty}^{\infty} N(\ell n\tau)\, e^{-t/\tau}\, d\, \ell n\ \tau \tag{11}$$

For both the internal friction and the anelastic creep the data analysis has become considerably more complex for a relaxation time spectrum compared to a single time. It is now necessary to unfold the integral equations to obtain the spectrum. Eqs. (8), (9), and (11) are Fredholm equations of the first kind. Such equations typically present difficulties because the problem may be ill posed so that there may be no solution or if a solution exists, it may not be unique. Also, even if the problem is well posed it may be ill conditioned because the random experimental error of the measurement may cause widely varying solutions. An important part of the analysis which follows will be to determine the extent to which experimental error affects the calculated $N(\ell n\ \tau)$ spectrum. Also since the integral equations each have different kernels and the unfolding can be markedly sensitive to the kernel, it is important to validate the procedure over various regimes for each kernel.

Direct Spectrum Analysis Method

The unfolding method to be described is referred to as Direct Spectrum Analysis (DSA). It involves making a sum approximation of the integral and then using a modified nonlinear regression rather than a linear least squares technique, thereby avoiding the highly oscillatory solutions which tend to occur with the latter with an increased number of bins (i.e., maximum index for the summation). It is equally applicable to the internal friction and the anelastic creep analyses. In the discussion which follows the emphasis will be upon analysis of internal friction results. A detailed description and validation of the method for the first-order kinetics of anelastic creep has previously been published (2).

A key requirement of any method for unfolding an integral equation such as Eq. (10) is that the method give only approximate solutions since true solutions may not exist, especially because of the random experimental error in the measurement. We then seek to establish that these approximate solutions are indeed unique. This is done by using DSA to analyze internal friction data which have been generated from a known $N(\ell n\ \tau)$ spectrum and to which random experimental error has been added. The comparison between the approximate solution from the DSA and the input $N(\ell n\ \tau)$ distribution function then allows validation of the method.

To obtain the DSA approximation of $N(\ell n\ \tau)$ we first determine the range of τ over which the spectrum will be considered, i. e., we specify the lower and upper τ limits, τ_s and τ_f, respectively. As an initial approximation a wide range is chosen, then an analysis is done. Subsequently the spectral limits may be adjusted keeping the upper and lower limits so that there is room for the tail regions of the spectrum. These limits then become the integration limits in Eq. (10). We next divide the range of log τ into n bins of equal width $\delta\ \ell n\ \tau = \ell n(\tau_f/\tau_s)/n$ and designate that the relaxation time associated with the i^{th} bin will be τ_i, the midpoint value (log scale) of the bin. The number of bins, n, which is chosen depends upon the resolution that may be required for the particular spectrum; typically $10 < n < 100$, but with the constraint $n \leq m$, where m is the number of data points.

For m data points and n bins the sum approximation of Eq. (10) gives

$$\tan\phi(\omega_j) \cong \Delta \sum_{i=1}^{n} A_i \frac{\omega_j\tau_i}{1+(\omega_j\tau_i)^2}, \quad (j=1,m),\ (n\leq m) \tag{12}$$

Here, the relaxation strength Δ is defined by Eq. (10a) and

$$A_i \equiv N(\ell n\ \tau_i)\,\delta\ \ell n\ \tau \tag{12a}$$

is the fractional contribution to the total relaxation from the i^{th} bin, $N(\ell n\ \tau_i)$ is the spectral amplitude of the i^{th} bin, and $\delta\ \ell n\ \tau$ is the previously defined bin spacing. Eq. (12) is the same equation that Nowick and Berry give in discussing multiple relaxation with descrete spectra (1). When we apply this same bin method and sum approximation to analysis of anelastic creep, Eq. (11) becomes

$$\Psi(t_j) \cong 1 - \sum_{i=1}^{n} A_i \exp(-t_j/\tau_i), \quad (j=1,m),\ (n\leq m) \tag{13}$$

where A_i has the same definition as in Eq. (12a). Thus for either kind of anelasticity experiment the goal of the analysis is to obtain the A_i in Eqs. (12) or (13).

At this point the DSA method makes a significant departure from traditional unfolding methods. Although Eqs. (12) and (13) describe a linear set of equations which can be solved for the A_i by standard techniques e.g., linear least-squares, a modified nonlinear regression least-squares method is used in order that the approximate solution not become highly oscillatory. This oscillatory behavior is a well known difficulty with solutions to this type of problem. It tends to occur when the number of bins is set large enough to be useful for resolving details in the spectrum (roughly $n > 10$). With increasing n the oscillations in the A_i tend to become extreme and produce A_i values which are either positive or negative and which have absolute values which are orders of magnitude greater than the expectation values. This tendency is due to the low amplitude high frequency noise which is present because of the random experimental error. The oscillatory solution is prevented by the combined use of the iterative nonlinear regression and the constraint $A_i \geq 0$. (In some cases the constraint $A_i \geq \epsilon$, where ϵ is some small negative number of order -10^{-4}, was used; only negligible differences were observed in the results using this instead of the zero constraint.) The combination of the iterative method and the constraint prevent highly oscillatory solutions because between successive iterations the A_i do not change markedly and thus can be prevented from taking values which with later iterations will lead to the large negative values and concomitant oscillations.

The nonlinear regression method which is best suited to the analysis we have described is a modified Levenberg-Marquardt algorithm (5). It has an advantage over other nonlinear regression methods because it has the capability of varying the multiplying factor for adjusting the Levenberg parameter and thus decreasing the number of iterations. Even with this improvement the method tends to require a relatively large number of iterations, often more than 10^3 depending upon the convergence criteria. Several different termination criteria were used. With the preferred one a tolerance is chosen (typically tol = (machine precision)^r with $0.50 \leq r \leq 99$) and then termination occurs when the estimate of the relative error between A_i and the solution is less than tol for all A_i.

Either of two methods were used to force the constraint $A_i \geq 0$. With the first, a substitution method, a non-negative function is substituted for A_i and then after iteration is complete the A_i are back-calculated. With the second method the constraint was obtained by modification such that any $A_i < 0$ is set equal to 0. This method, although it is actually an improper use of the algorithm for the nonlinear regression because it modifies the solution between iterations, is workable because the drastic oscillatory behavior requires several iterations to develop so that after a given iteration any $A_i < 0$ is still small enough so that setting it to zero does not appreciably alter the iterative approach. This modification method is the better of the two and has been used in all the examples which follow. For a more detailed discussion of the use of this constraint and the termination criteria the reader is referred to Ref. (2).

Validation of the Method

The validation method consists of generating artifical sets of anelastic response data from known relaxation time spectra, adding random (Gaussian) experimental error with a desired standard deviation σ to the data, and then applying the DSA method to the data to test how well the input spectrum is recovered. In the examples which follow the input distribution of relaxation times was either a single or a combination of several lognormal (Gaussian in log τ) distributions given by

$$N(\ln \tau) = 1/(\beta \sqrt{\pi}) \exp(-\ln(\tau/\tau_m)/\beta)^2 \qquad (14)$$

which is a single-peak distribution centered and symmetrical about a logarithmic mean relaxation time τ_m and with width parameter such that the full width at 1/e of the maximum is 2β. Multiple-peak input spectra were also checked. The data were generated from a spectrum composed of linear combinations of single lognormal distribution functions. Such a spectrum requires an extra parameter α which gives the fractional contribution to the total spectrum of each lognormal peak.

Internal Friction

Single Peak Spectra. Fig. 1 shows an example of an internal friction curve which has been generated by computer. In this figure tan ϕ/Δ, the internal friction normalized by the relaxation strength is plotted logarithmically against frequency on the top scale and against reciprocal temperature on the bottom scale. As previously discussed, these plots are equivalent and differ by a scale factor $Q/2.3k$ according to Eq. (5). Thus the top scale is for internal friction measured isothermally at constant relaxation time, $\tau = 1.0$s, while the bottom scale corresponds to measurements at constant frequency, $\omega = 1.0\ s^{-1}$, with the

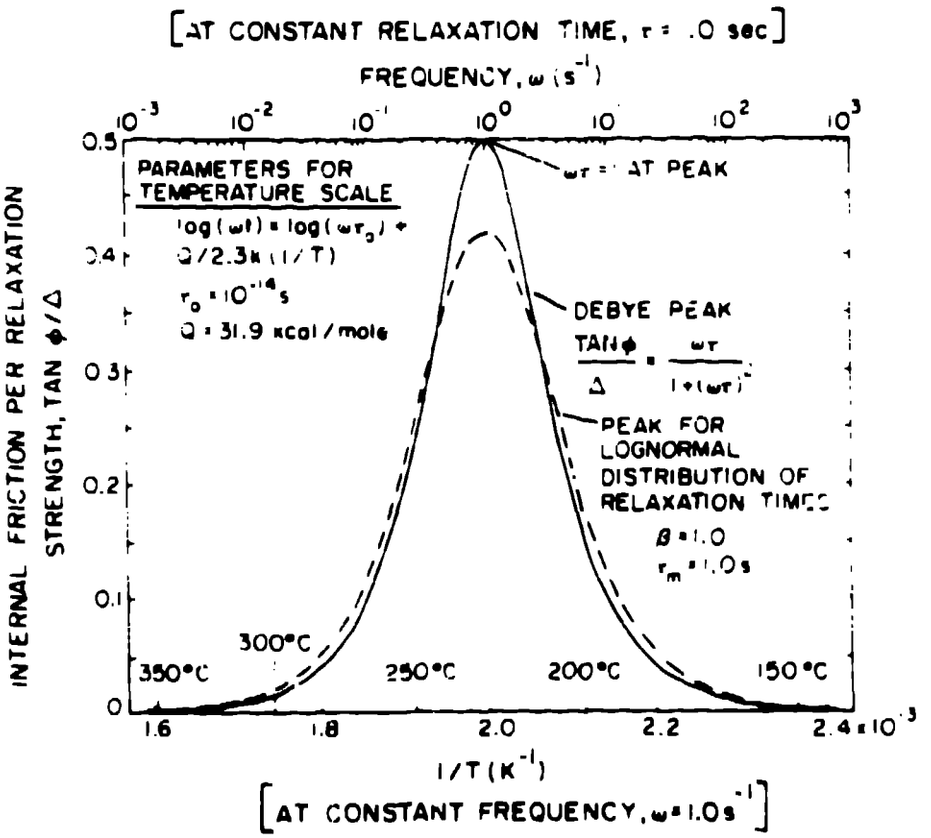

Figure 1. Internal friction (normalized by the relaxation strength) versus both frequency (log scale) and reciprocal temperature. The solid curve is for a Debye peak, i.e., for a single relaxation time. The dashed curve is for a lognormal distribution of relaxation times as described in the text. The peaks are symmetrical on both the log frequency and the 1/T scales. The values shown for τ_0 and Q were chosen to give a convenient scale factor and peak position for the 1/T plot.

Arrhenius relation being given by the pre-exponential $\tau_0 = 10^{-14}$s and the activation energy Q = 31.9 kcal/mole. The more narrow of the two internal friction peaks in Fig. 1 is a Debye peak (single discrete relaxation time) while the broader peak is calculated from a single lognormal distribution of relaxation times with midpoint $\tau_m = 1.0$s and width $\beta = 1.0$. The close similarity of these two curves in Fig. 1 which have actually markedly different distribution functions provides an indication of the appreciable difficulties involved in the problem of obtaining the relaxation time spectrum. Also, it should be pointed out that the analysis method must be sensitive to subtle differences in the overall shape of the curve irrespective of the scale factor for vertical scale. This is because in any experimentally measured situation the magnitude of the relaxation strength Δ is unknown so that the measured quantity is tan ϕ instead of the normalized quantity tan ϕ/Δ shown in Fig. 1.

Fig. 1 shows a continuous plot of the normalized internal friction. Discrete data pairs which have been computer generated for analysis by the DSA method are shown in Fig. 2 for the same input lognormal distribution as in Fig. 1. In this and subsequent sets of computer-generated data to be analyzed, m = 50 data points have been generated. Also, to provide realistic simulation of experimental results, these data have been chosen at unequal intervals on the log ω or 1/T scale and random (Gaussian) experimental error has been added to the exactly-calculated data points. In this and all subsequent internal friction validations in this paper, the standard deviation for the fractional experimental error was chosen as $\sigma = 0.01$, which is a generous estimate of the fractional error in a typical measurement. Evidence for the random scatter in the data may be observed in Fig. 2, especially in the region of the maximum internal friction.

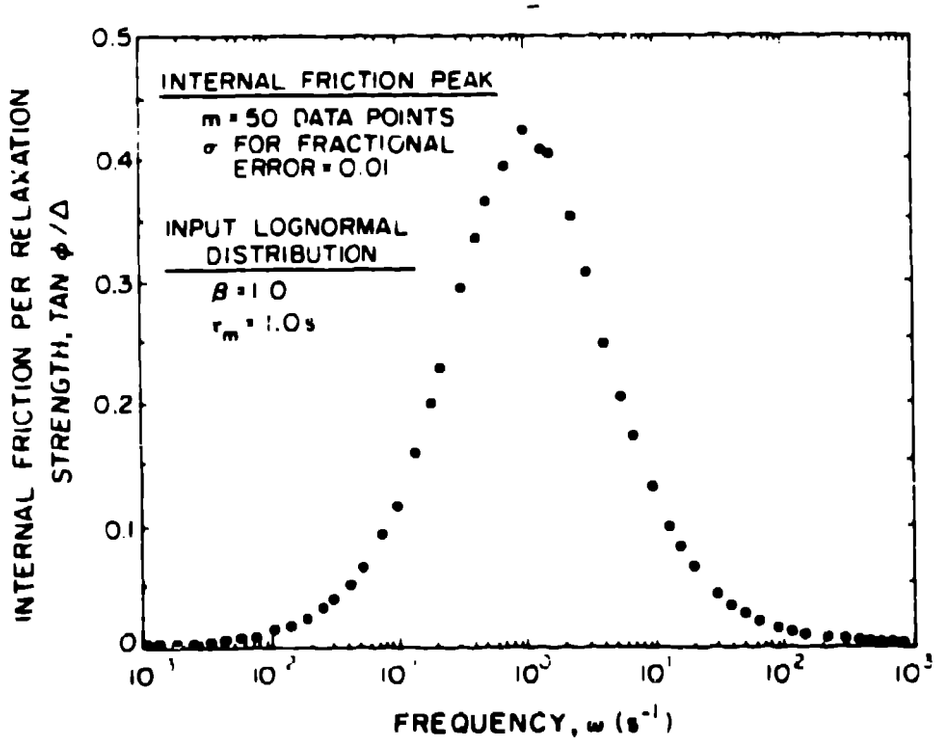

Figure 2. Computer generated internal friction versus frequency (log scale) plot for the same lognormal distribution peak shown in Fig. 1, but with random fractional error having standard deviation $\sigma = 0.01$ added to the data

The starting condition for DSA of the data in Fig. 2 is shown in the histogram of Fig. 3. Here the spectral amplitude of the i^{th} bin, $N(\ell n\ \tau_i)$, is plotted versus the relaxation time on a logarithmic scale. The upper and lower spectral limits as are shown by the dotted vertical lines have been chosen as $\tau_s = 0.03s$ and $\tau_f = 30s$. The number of bins has been set as $n = 40$, and as shown the spectral amplitude is initially set equal in each bin, $N(\ell n\ \tau_i) = 1/\ell n(\tau_f/\tau_s) = 0.1448$ such that the area of the histogram is 1/2.303 (area of 1.0 plotted on a natural logarithmic scale). At this point the system is ready to begin the iteration process to obtain approximate solutions for the A_i according to Eq. (12).

The DSA histogram approximation after 500 iterations of the data in Fig. 2 is shown in Fig. 4. Also shown in Fig. 4 as a smooth solid line is the input spectrum used to generate the data of Fig. 2. The histogram has an area such that $\Sigma A_i = 0.999$ in excellent agreement with the definition of A_i as the fractional contribution to the relaxation from the i^{th} bin. Qualitatively comparing the output histogram with the input distribution function in Fig. 4 we see that the histogram approximation provides good reproduction of the original spectrum judged by amplitude, width, position, area and general shape. This result that the DSA method is capable of approximating the input spectrum with such good accuracy with only 50 data points and with random fractional error of roughly 1% is strong evidence for the capability of the method. It is, in fact, somewhat unexpected that a set of data to which appreciable disorder in the form of random noise (experimental error) has been introduced can be processed to re-establish the original information (input spectrum) which is inherent in the system. This ability to filter the high frequency noise as a part of the process of deconvoluting the data to obtain the original spectrum is an important strength of the DSA method.

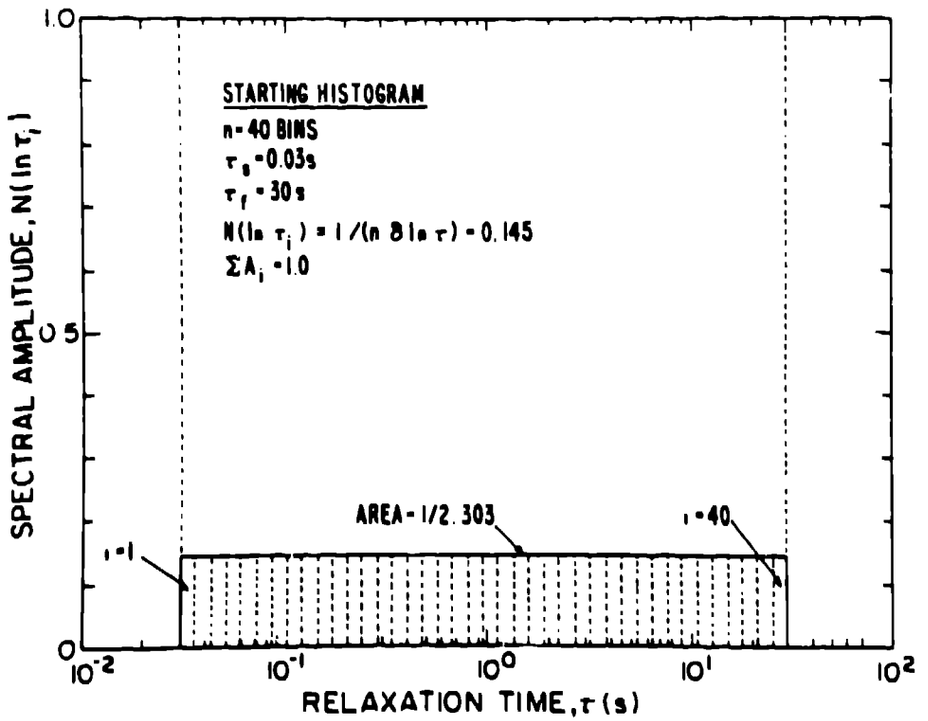

Figure 3. Histogram for the start of the nonlinear regression analysis calculation of relaxation time spectrum. This starting histogram is divided into $n = 40$ equally spaced (log scale) bins. The spectral limits τ_s and τ_f have been chosen to include the expected full range of the input distribution of relaxation times.

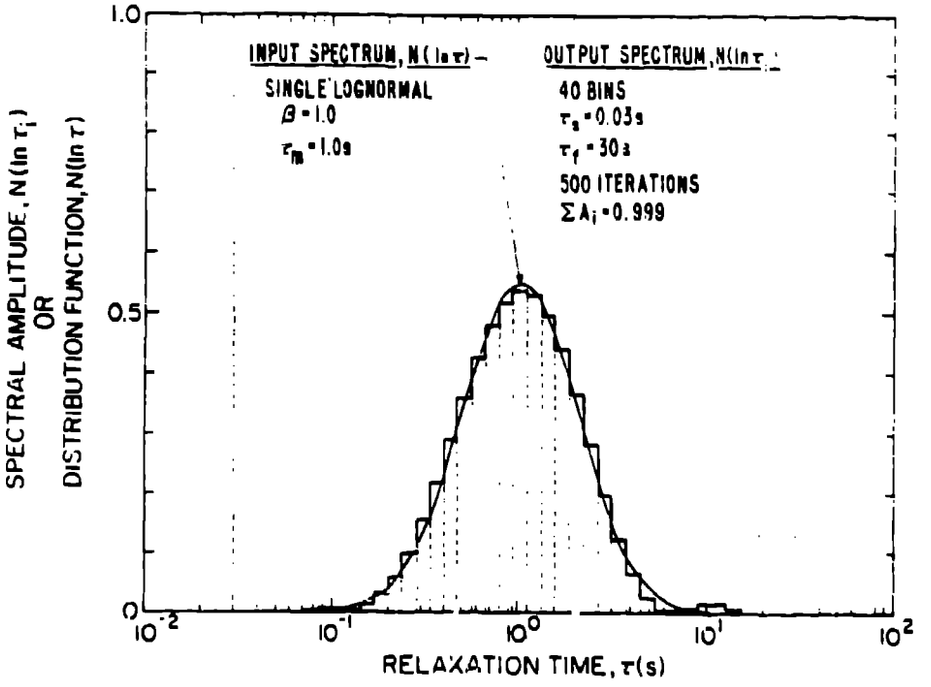

Figure 4. Histogram of Fig. 3 but after 500 interations using the DSA method. The histogram shows good agreement with the input spectrum (solid line) used to generate the data of Fig. 2.

A more quantitative measure of the agreement between the input spectrum and DSA approximation is desirable. This may be obtained by determining the position and width of the histogram by fitting a lognormal curve through the output histogram to obtain the mean relaxation time τ_m and the width parameter β. The results for such a fit to the data of Figs. 2 and 4 are shown in Table I. Here we see (for $\beta = 1.0$) that the position of the output spectrum is 1.021s compared with 1.0s for the input. Similarly the width parameter β has been reproduced within roughly 3%.

Table I. Input and Output Parameters for Lognormal Relaxation Time Spectra

INPUT[a]			OUTPUT (DSA)[b]				COMPARISON[c]		
τ_m(s)	β	Area	τ_m(s)	β	ΣA_i	Iteration	τ_m(%)	β(%)	ΣA_i(%)
1.0	0.1	1.0	0.929	0.290	1.000	500	7.1	190	0
1.0	0.3	1.0	1.006	0.289	1.005	500	0.6	3.7	0.5
1.0	1.0	1.0	1.021	1.030	0.999	500	2.1	3.0	0.1
1.0	2.0	1.0	1.015	1.975	1.001	200	1.5	1.3	0.1
1.0	3.0	1.0	0.848	3.185	0.995	100[d]	15.2	6.2	0.5

[a]Used to generate internal friction data with 50 data points to which random fractional experimental error with standard deviation $\sigma = 0.01$ is added.

[b]From direct spectrum analysis of the computer-generated internal friction data using 40 bins followed by a fit to a lognormal distribution.

[c]Percent difference between input and output parameters.

[d]Smoothed data.

A final feature of the DSA histogram approximation in Fig. 4 which should be mentioned is the existence of the small sidepeaks which occurs at roughly 10^{-1} and 10s. These peaks tend to show up in most DSA results. They tend to have magnitudes which increase with increasing experimental error (or for the anelastic creep analysis, when there is error in the measurement of the initial and final values for the anelastic strain). Also, these sidepeaks are stable for a given calculation in that they do not change with further iteration. Interestingly, these peaks tend to vary markedly in position, shape, and amplitude depending upon the choice of the calculation parameters τ_s, τ_f and n. The main spectral peaks, on the other hand, do not tend to show this variation. This result that the input spectrum is reproduced consistently independently of the calculation parameters, while the sidepeaks are not, is important since it provides the capability of determining whether a part of the spectrum approximation is intrinsic or merely a non-reproducible artifact of the calculation.

Effect of Width of Spectrum. It is desirable to know the capability of the DSA method for determining spectra of various widths. This was done by generating and analyzing sets of internal friction data from input spectra with various β, but with constant τ_m = 1.0s. The range of β was 0.1 to 3.0. Each of the data sets was again generated with m = 50 data points of tan $\phi(\omega)/\Delta$ vs ω spaced at unequal intervals of log ω. Also, the same standard deviation, σ = 0.01, was used for the random fractional error added to the tan ϕ/Δ values. The internal friction data for β = 0.1 are nearly undistinguishable from data for a single discrete relaxation (Debye peak), while those for β = 3.0 give an internal friction peak which is more than twice the width of a Debye peak of the same height, see Fig. 5.

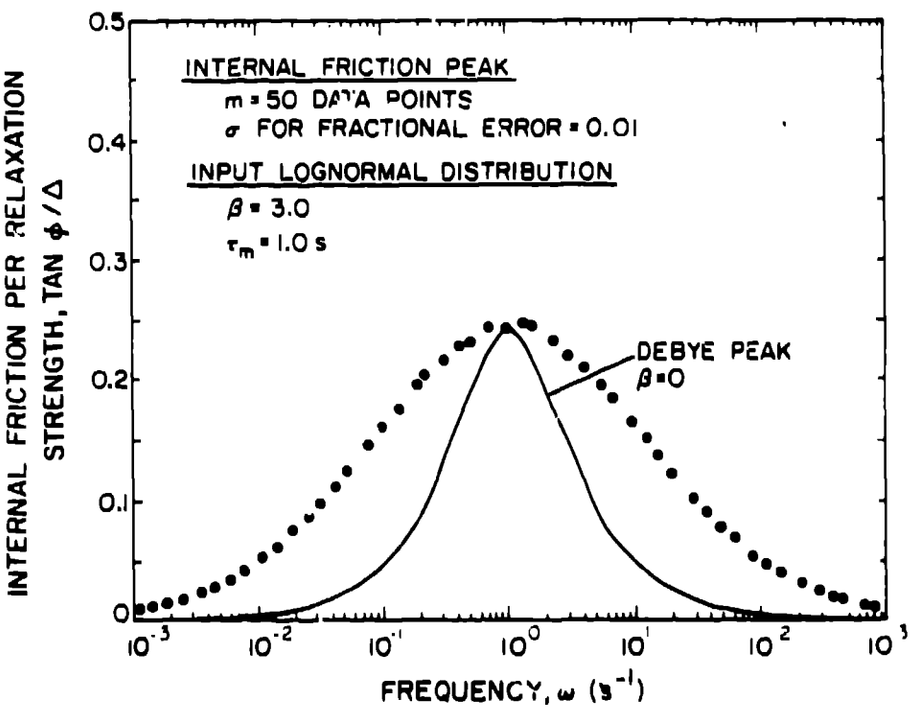

Figure 5. Data for internal friction versus frequency for a lognormal input distribution of relaxation times having β = 3.0. Random fractional error with standard deviation σ = 0.01 have been added to the data. A Debye peak (solid line) is shown for comparison.

The capability of the DSA method for resolving very narrow relaxation time spectra from the corresponding internal friction data varies depending upon the spectral width. Typically it is not as good as was demonstrated for the relatively wide spectrum ($\beta = 1.0$) of Fig. 4. This is shown in Fig. 6a in which the narrow input spectrum for $\beta = 0.1$ has a maximum amplitude above 5.0, while the calculated histogram approximation, although it is in the proper position and has a shape which is nearly Gaussian, is too wide by more than a factor of three and has a maximum amplitude of less than 2.0. The histogram approximation does however have a spectral area $\Sigma A_i = 1.0003$ which is satisfactory when compared to the expectation value of unity. When the width of the input spectrum is increased from $\beta = 0.1$ to $\beta = 0.3$, the anlaysis method is able to estimate the input spectrum with good accuracy. This is shown in Fig. 6b; here the histogram approximation coincides well with the $\beta = 0.3$ input spectrum. As indicated, the histogram was created using 500 iterations with the spectra limits adjusted to be wider than for the narrower $\beta = 0.1$ peak in Fig. 6a.

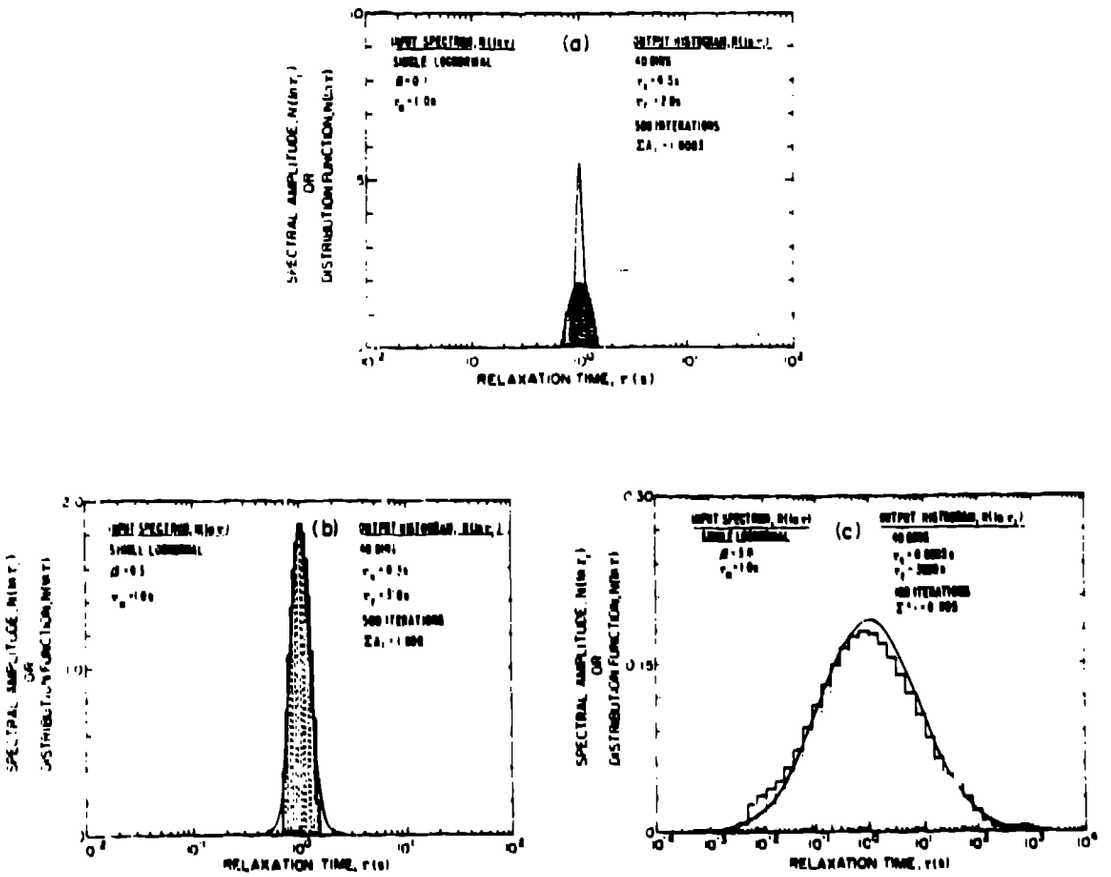

Figure 6a to 6c. Input spectra (solid lines) and output histograms for internal friction data generated from single lognormal distributions of various widths: (a) $\beta = 0.1$, (b) $\beta = 0.3$, and (c) $\beta = 3.0$. Note the scale differences, especially for the most narrow distribution ($\beta = 0.1$) and the very wide distribution ($\beta = 3.0$).

When the input spectrum becomes extremely wide, such as for $\beta = 3.0$ yielding the internal friction data of Fig. 5, the DSA method again is able to reproduce the input spectrum with acceptable accuracy, see Fig. 6c. Here it may be seen that the coincidence between the input spectrum and the output histogram is satisfactory but not as good as for $1.0 \geq \beta \geq 0.3$. Note that in Fig. 6c, because of the wide spectrum the horizontal scale covers a range of log τ which is twice that of the previous figures. To obtain the results for the wide spectrum in Fig. 6c from the internal friction data of Fig. 5, it was desirable to set the spectral limits as $\tau_s = 0.0003$s and $\tau_f = 3000$s, a spectral breath of seven decades. Also, for this anlysis it was necessary to smooth the data to remove some of the high frequency noise of the simulated experimental error. Without this smoothing operation the oscillatory solutions previously discussed tend to develop resulting in multiple sharp peaks, the envelope of which, has the shape of the histogram in Fig. 6c. The smoothing operation consisted of sequentially least-squares fitting of either a 2nd or 3rd degree polynomial to segments of the data consisting of from 7 to 11 data points and thus redetermining each data point as the one on the polynomial curve. The smoothing operation apparently is required when there is both appreciable scatter in the data and the spectrum is relatively wide ($\beta > 2.0$). When it was used on data with $\beta \leq 2.0$ but with the same fractional experimental error, it was shown not to change the output histogram appreciably.

As was done for the histogram results of Fig. 4, a quantitative indication of the success of the DSA method for analysis of internal friction data derived from relaxation time spectra with a single lognormal peak of varying width was obtained by fitting a lognormal distribution to the output histogram. The lognormal parameters obtained from this fitting are given in Table I for the histograms shown in Fig. 6 plus an additional result for $\beta = 2.0$. The last columns of Table I give the percent differences between the input lognormal parameters and those obtained from the output histogram. Here it may be observed that except for the very narrow input spectrum with $\beta = 0.1$ the position, width, and area (ΣA_i) of the DSA histograms are within roughly 10% of the input values; this appears to be satisfactory for most applications. Also, it may be observed in Table I that when the spectral width becomes large ($\beta > 2.0$ for this case) the uncertainty in the peak position and width is markedly increased. For applications in which wide spectra are involved special care will be necessary to validate the DSA results.

Multiple Peak Spectra. One of the key needs in analyzing internal friction data is the capability for determining whether a given anelastic response is due either to a single relaxation process with a somewhat broad distribution of relaxation times or to two or more processes each with relatively narrow or nearly-discrete relaxation times. This may be particularly important in situations in which it is desirable to know whether there is more than one mechanism controlling the reaction kinetics. Thus we now investigate the capability of the nonlinear regression analysis method to unfold more complex spectra. To do this $\tan \phi/\Delta$ vs ω data were again generated with $m = 50$ data points from $N(\ell n\, \tau)$ vs log τ distribution functions which had more than one peak. Subsequently random fractional experimental error was added with $\sigma = 0.01$.

In Fig. 7 internal friction data are shown (peak B) which have been generated using a distribution function with two equally weighted lognormal distributions, each with $\beta = 0.5$ (which is relatively narrow) and with mean relaxation times which are a factor of four apart ($\tau_{m1} = 0.5$s and $\tau_{m2} = 2.0$s). These internal friction data points may be compared with those of Fig. 2 for the single lognormal distribution shown in Fig. 4 which are replotted in Fig. 7 as peak A. It may be seen in Fig. 7 that only small differences exist between the two sets of data even though each set was generated from markedly different relaxation spectra. Specifically, the peak heights and widths are nearly the same, and there are only slight differences in the tail portions. Their close similarity serves again to point out the difficulty of the unfolding problem . . . how to reconstruct very different input spectra from data which appear to be very similar. The results from the DSA of internal friction peak B in Fig. 7 are

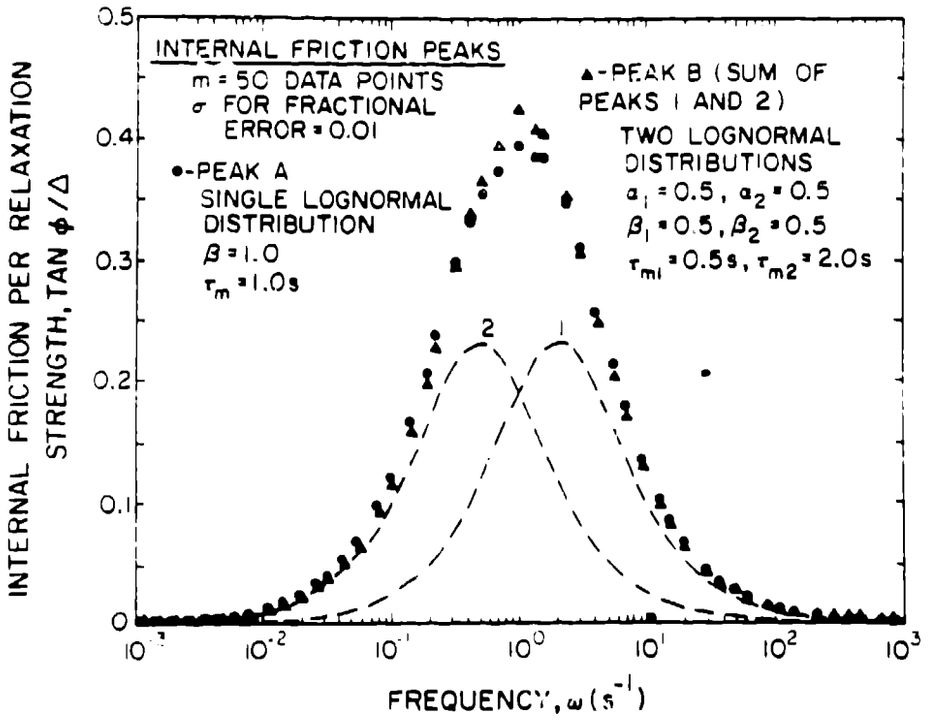

Figure 7. Data for two internal friction peaks plotted versus frequency. Peak A is from a single lognormal distribution (same as Fig. 2). Peak B is made up of peaks 1 and 2 which are from two different lognormal distributions with parameters as indicated. The close similarity of the two internal friction peaks is indicative of the difficulty of the unfolding operation required to obtain the two very different inout spectra. Random fractional error with $\sigma = 0.01$ has been added to both sets of data.

shown in Fig 8 as the usual histogram approximation of the spectrum. Also shown as a solid line is the 2-peak input distribution function. Comparing the histogram with the input spectrum we observe that the unfolded approximation is quite good. Importantly, the two peaks have been resolved even though they are close enough together so that they overlap, see dotted lines for separate contributions of the two input spectra. Also, the 40 bin approximation gives good reproduction of the height and position of the input distribution. Interestingly, the peak centered at the short relaxation time $\tau_{m1} = 0.5s$ is reproduced better than the one at the longer time, $\tau_{m2} = 2.0s$. Also, the histogram peak at the longer time is not centered as well with the input peak so that the two differ by roughly 50% in position. This tendency for the DSA results to produce adjacent peaks with greater spread than exists with the input distribution was found to be the case for many of the multiple-peak relaxation spectra which were investigated, especially when two of the peaks were relatively close together. Typically, it resulted in shifts in the peak position of 10 to 25%. This tendency may not always be a serious drawback since the capability to resolve separate peaks which are in close proximity and thus demonstrate the existence of separate intrinsic processes is typically more important.

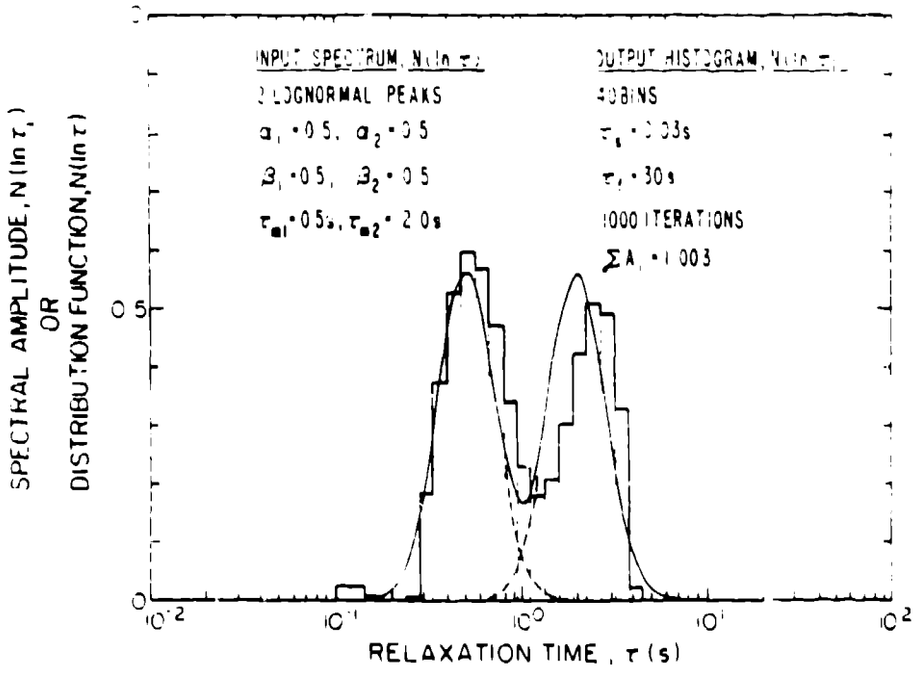

Figure 8. Input spectrum (solid line) and calculated output histogram for peak B of Fig. 7. The DSA histogram shows that the two overlapping peaks of the input distribution function have been resolved.

As a final test of the capability of the DSA method to reproduce multiple-peak spectra we consider the analysis of the internal friction results shown in Fig. 9. Here is shown an internal friction peak ($m = 50$, $\sigma = 0.01$) which is the superposition of the four separate peaks shown as dotted lines. These four peaks are each determined by relatively narrow lognormal distributions ($\beta \leq 0.5$) which have mean relaxation times differing by factors of 4 or 5. The test of the method is how well it will be able to retrieve the original 4-peak input spectrum by analysis of the 50 internal friction data points after random fractional experimental error with $\sigma = 0.01$ has been added. The result of this calculation using 500 iterations is shown as the histogram in Fig. 10 along with the input $N(\ln \tau)$ distribution function used to generate the data. (Here the dashed lines are the seperate spectral contributions and the solid line is the additive curve.) Fig. 10 shows that the histogram provides a very good approximation of the input spectrum. All four of the original peaks have been resolved and have amplitudes, positions, and shapes which agree well with the original distribution function. This capability to replicate the fine structure of a 4-peak input spectrum, even for a peak with fractional contribution of 0.15 (peak #1), is gratifying since it should be sufficient to meet most needs in practice.

Effect of Calculational Parameters. There are three parameters which are chosen for any given DSA calculation, the number of bins, n, and the spectral limits, τ_s and τ_f. In general the results of the calculations were not found to be changed appreciably (< 5% in the width, position, and amplitude of the main spectral peaks) by the choice of these parameters. Often it is desirable to choose a large number of bins since the spectral resolution is improved. Usually this choice is a compromise between desired resolution and available computer time. The latter can be an important consideration since these calculations typically require in the neighborhood of 500 iterations and the calculation time per

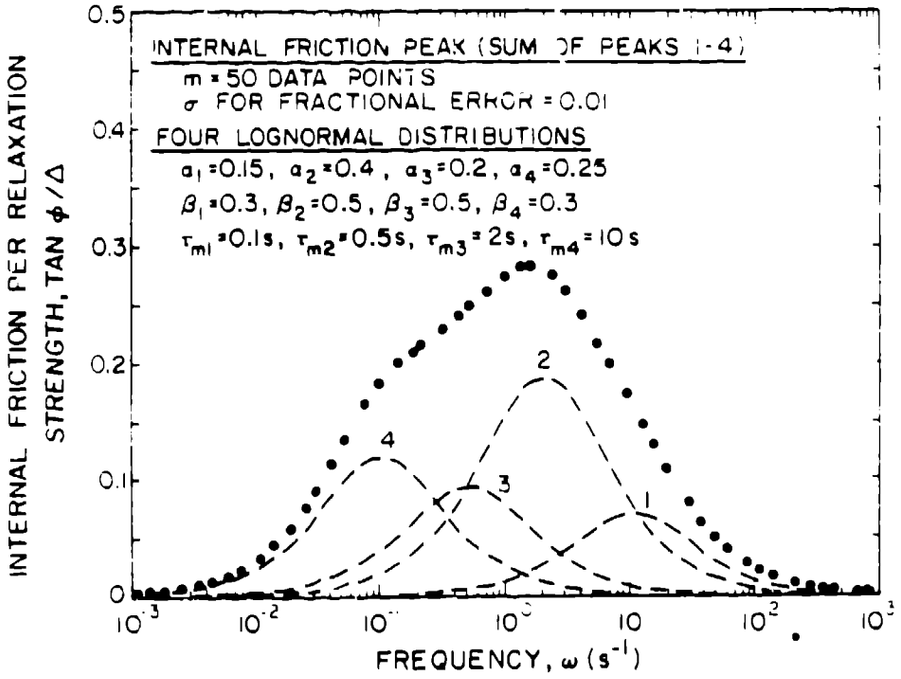

Figure 9. Data for broad internal friction peak which is a combination of peaks 1-4 which are defined by four different lognormal distributions with parameters as indicated. Random fractional error with $\sigma = 0.01$ has been added to the data.

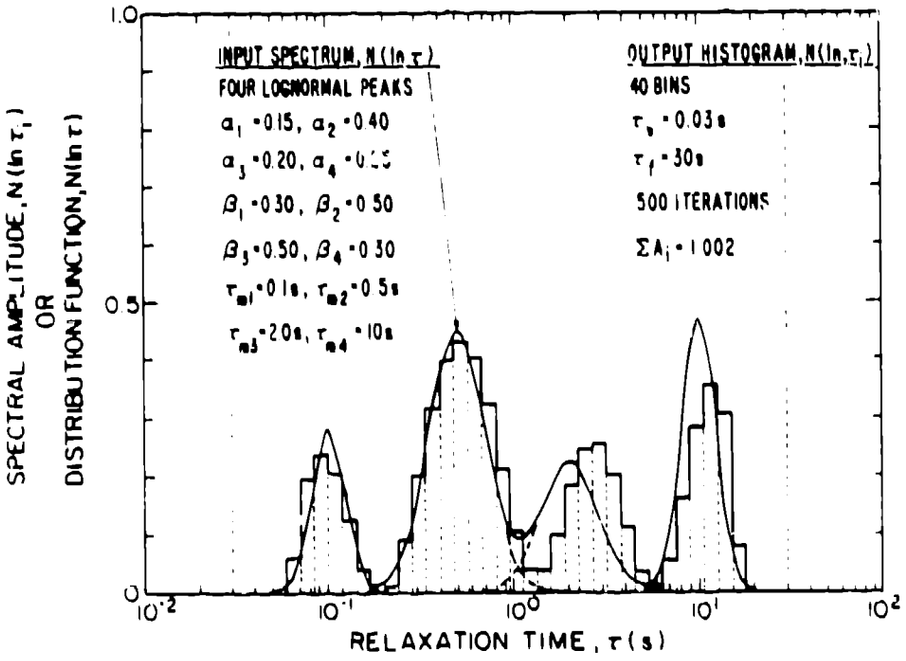

Figure 10. Input spectrum (solid line) and calculated output histogram for data in Fig. 9. The histogram shows that the four nearly-overlapping peaks of the input spectrum have all been resolved.

iteration increases roughly as the square of the number of bins. As mentioned earlier, the choice of these parameters was found to markedly affect the position and amplitude of the small sidepeaks and thus by repeating the analysis with different choices for these parameters, variations in the sidepeaks allowed them to be distinguished from the main peaks which are relatively unaffected.

Convergence and number of iterations. The relatively large number of iterations which were used in the examples given so far were not always required. For instance, with no experimental error added to the data it was found for both internal friction and anelastic creep data that the sum of the squares of the residuals approached the machine accuracy (chosen as the termination criteria) after less than 50 iterations. Typically, more iterations were required for data with greater amounts of experimental error. In general, it was found that initial convergence was relatively rapid while final convergence was slow. Also, the rate of convergence and the final convergence values depended strongly, but in no systematic way, upon the choices for τ_s, τ_f, and n. This again serves to emphasize that the method gives approximate, as opposed to exact, solutions. The approximate solutions, although they are not unique because they depend upon the choice of calculation parameters, in all cases examined gave results which are relatively close to the input spectrum.

Anelastic Creep

Validation of the DSA method for the first-order kinetics of anelastic creep have already been discussed in detail (2). The following will review main points of the original discussion particularly with regard to effects of the magnitude of experimental error upon the calculated spectra. Again, the purpose of the calculation will be to approximate the original relaxation time spectrum, but now with this spectrum controlling the anelastic creep response. As before, the DSA method will do this by calculating the A_i, except the appropriate equation will be Eq. (13), and the data to be used in validation of the method will be fractional anelastic creep $\psi(t)$ vs t.

Effect of experimental error. Fig. 11 shows a set of $\psi(t)$ vs time (log scale) data with m = 250 and no experimental error. These data have been calculated from an input $N(\ell n\ \tau)$ distribution function which is shown in the same figure. This is a lognormal distribution function with width parameter $\beta = 1.0$ (as in Fig. 4) and centered at $\tau_m = 10^4$s. The output histogram of $N(\ell n\ \tau_i)$ after 31 iterations using 39 bins is shown in Fig. 12. For this calculation the constraint $A_i \geq \epsilon$ with $\epsilon = -0.0005$ was used instead of the $A_i \geq 0$ constraint since it gave more rapid convergence. Also shown in Fig. 12 are the parameters obtained by fitting a lognormal distribution to the histogram result. When these parameters are compared to the corresponding ones of the input spectrum (also shown in Fig. 12) the agreement is extremely good, better than 0.2% for all parameters. Such good agreement obtained after relatively few iterations was found when the data had no simulated experimental error added.

To access the capability to reproduce input spectra with experimental error added, a "worst case" set of data were generated by adding random error with standard deviation $\sigma = 0.05$ (i.e., roughly 5% error) to the data shown in Fig. 11. These anelastic response data are shown in Fig. 13. When these data were analyzed using DSA with n = 39 bins and $\epsilon = -0.0005$ the histogram shown in Fig. 14 was obtained. This histogram is a relatively good approximation of the original, especially considering the large amount of scatter in the data. A possible problem with this histogram result might be the relatively small sidepeak at the upper spectral limit; however, this sidepeak can be filtered out in a similar way as for the internal friction results by repeating the calculation with a different value for τ_s, τ_f, or n. As before, a quantitative measure of the agreement between the input spectrum and the

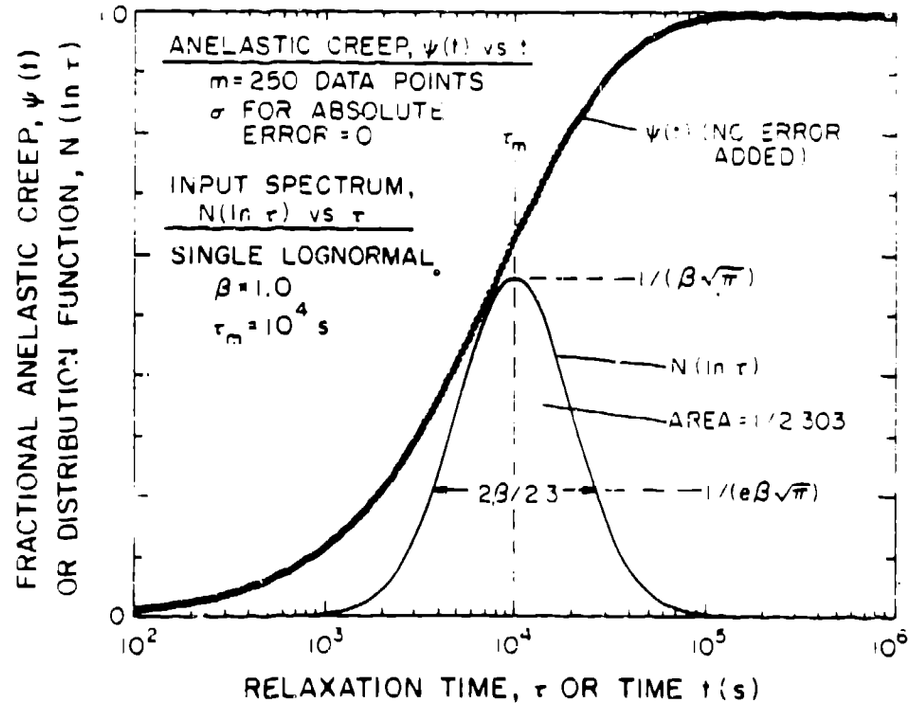

Figure 11. Computer-generated anelastic creep data of ψ(t) vs time (log scale) obtained from the input lognormal spectrum of relaxation times shown in this same figure as the solid line plot of N(ℓn τ) vs τ(log scale). No experimental error has been added to the data.

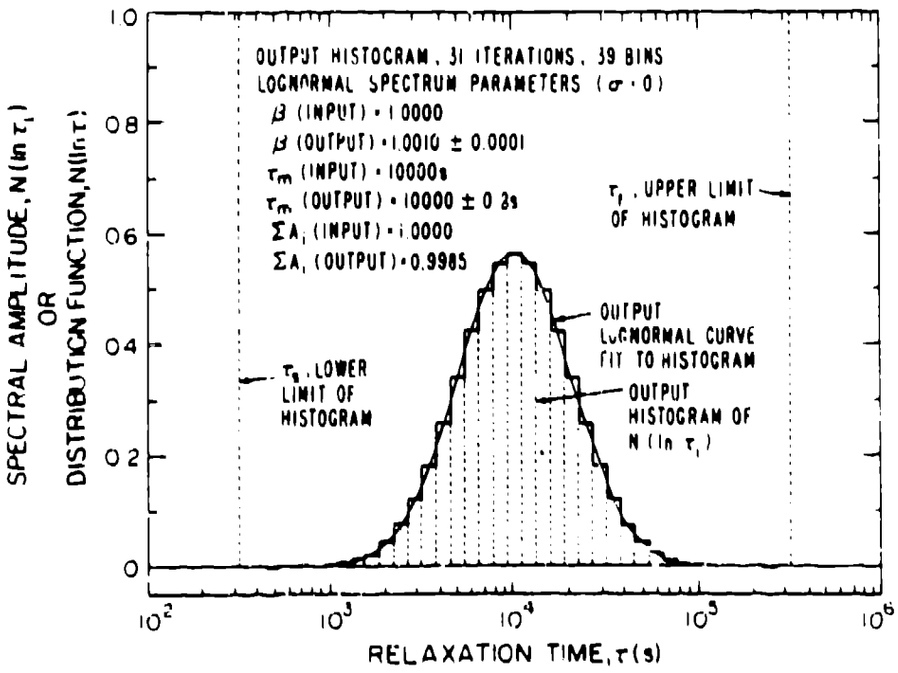

Figure 12. Output histogram estimate of the input distribution function in Fig. 11 obtained by the DSA method applied to the anelastic creep results also shown in Fig. 11. The solid line is obtained by fitting a lognormal distribution to the histogram.

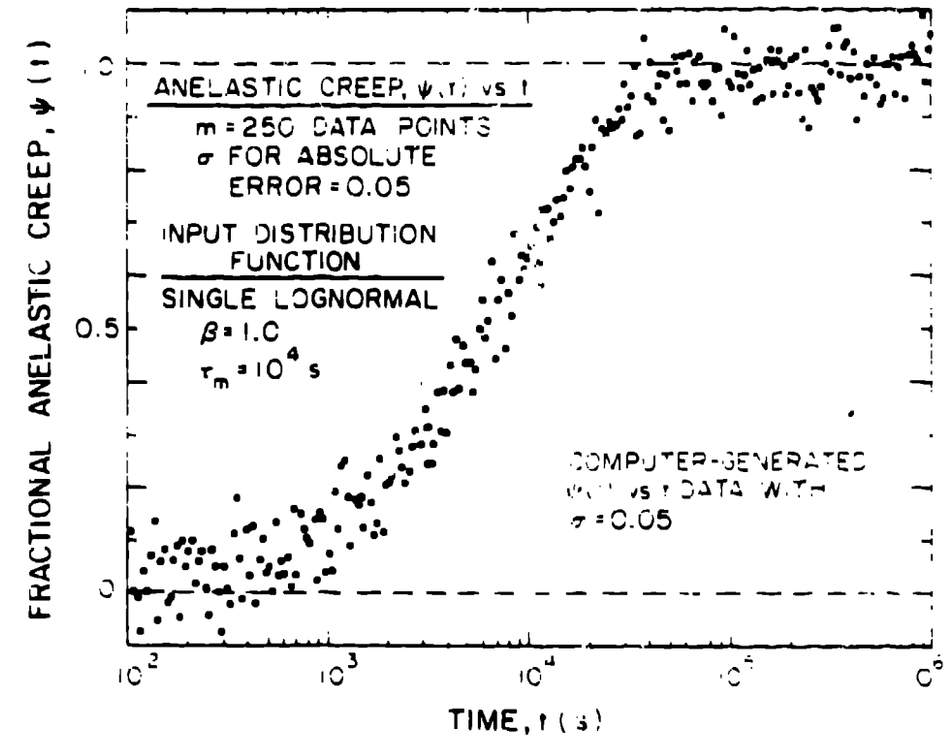

Figure 13. Same computer-generated ψ(t) vs time data as in Fig. 11, but with simulated experimental error obtained from a Gaussian distribution with σ = 0.05 added.

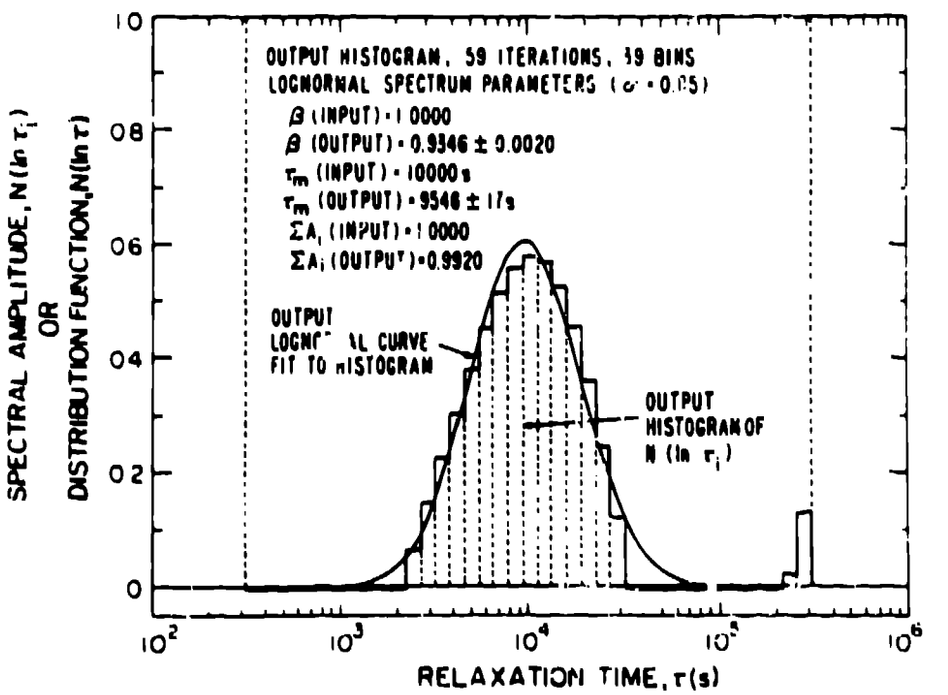

Figure 14. Output histogram (39 bins) and lognormal distribution fit to histogram (solid curve) after 59 iterations using the data of Fig. 13 with random experimental error having σ = 0.05 added.

histogram approximation has been obtained by fitting a lognormal distribution to the histogram. the resulting output spectral parameters. which are also shown in Fig. 14, agree with the input spectrum within roughly 6.5% for β, 4.5% for τ_m and 0.8% for the area.

Examination of these and other results from computer-generated data with varying amounts of experimental error show the following effects due to increased amounts of random error: (i) There is no systematic variation in the position, width, or shape of the histogram. (ii)The fine structural details such as the tails of the spectra tend to become obscured. (iii) The number of iterations required to reach the termination criteria is increased. (iv) the sidepeaks tend to become larger, but to still vary in position and amplitude with different choices for the calculation parameters.

Multiple peak spectra. As has already been discussed for the analysis of internal friction results, the validation of the DSA method for analysis of anelastic creep results has included investigation of effects due to multiple-peak input spectra (2). Some general findings of these investigations will be described.

Data were generated with m = 250 data points with the N ($\ell n\ \tau$) distribution composed of two overlapping lognormal peaks with mean relaxation times differing by a factor of 10. Subsequently, random error with $\sigma = 0.001$ was added to $\psi(t)$. Analysis of these data with up to n = 60 bins showed very satisfactory replication of the magnitude, shapes, and positions of the two-peak input spectra. Quantitatively it was found that the output spectral parameters (using a two-peak lognormal fit to the histogram) showed an average difference of less than 4% from the corresponding input parameters.

Similar investigations were made using single and double box distributions for the input spectra. This was done to test the capability of the method for analysis of data which were derived from other than a lognormal distribution. The box distribution in addition to the lognormal is discussed in detail by Nowick and Berry (1). It is a more stringent test of the DSA method than the lognormal because it has discontinuities. When data derived from box distributions were analyzed, the resulting histogram approximations gave good reproduction of the positions and relative magnitudes of input spectra for both single and double box distributions. However, as might be expected, there was difficulty reproducing the exact shape of the box, particularly at the sharp corners. This finding is in agreement with internal friction results for the very narrow sharp distributions with $\beta < 0.25$: apparently the DSA method can not easily resolve such fine detail. In some cases this resolution capability may be improved by increasing the number of bins. For applications of the method to spectra with fine structure it becomes particularly important to do validations in regimes which are applicable to the input spectra being investigated.

Other effects. Ref. (2) presents a fairly detailed investigation of how variation of the calculational parameters affects the DSA results for the analysis of anelastic creep. As previously discussed, for any given application, because the DSA result is only an approximation of the input spectrum, there is no unique output histogram. Thus the important thing to consider is how much this histogram varies when the parameters for doing the calculation are changed. Many cases were studied; no evidence was found for systematic variation in the solutions with changes in the calculational parameters. Also, in all cases the approximate solution histograms were good estimates of the input spectrum. The key point here is that the nonlinear regression least-squares algorithm gave approximate solutions which were close both to each other and to the known input spectrum when different calculational parameters were chosen. This finding that the DSA method does not produce incorrect approximations of input spectra is another important result of the validation.

One other point should be mentioned concerning the validation of the DSA method for use with anelastic creep data. It was found that the method has a better resolution capability for narrow input spectra when it is applied to the first-order kinetics of anelastic creep than it does for the Debye equation of internal friction. For instance, with anelastic creep it was shown to satisfactorily reproduce input spectra for a single lognormal peak with $\beta = 0.1$ (3) while, as we have shown here, for internal friction results the most narrow peak that was resolved had $\beta = 0.3$. Such a result is not unexpected; it merely reflects the well known effects of widely differing behavior of different kernels in the integral equation.

Internal Friction vs Temperature

As was previously pointed out in discussing differences between constant temperature and constant frequency internal friction experiments, it is experimentally desirable to do experiments while varying the temperature instead of the frequency. The discussions in the previous section validated the internal friction analysis method for frequency as the variable because this is more easily treated. Since this validation is for the Debye equation as a kernel, it is, however, equally applicable to cases in which temperature (or relaxation time) is the variable. Thus the validation need not be repeated. In the following discussion the relationships for analysis of relaxation processes in which internal friction is measured as a function of temperature will be described. This discussion will treat this problem without making the usual simplifying assumption that $J_1 \simeq J_u$. It will, however, assume that the variation of frequency with temperature is relatively small and thus can be ignored.

It is convenient at this point to consider two extremes in the distribution of relaxation times which governs the relaxation kinetics. These both arise naturally from the Arrhenius relation, Eq. (4). For a detailed discussion see Nowick and Berry (1). The first extreme to be considered is one in which the distribution arises only from a distribution in the pre exponential factor τ_0. Thus this distribution has only a single activation energy. The second extreme applies to the opposite condition, that the distribution is due completely to a distribution of activation energies. Thus for this distribution there is a constant pre-exponential factor τ_0. In practice a combination of these two conditions may exist, but for the analysis it is useful to assume one or the other.

Distribution of τ_0 Only

For this case we consider the distribution $N(\ell n\ \tau_0)$ which is the relaxation time spectrum of pre-exponential Arrhenius factors. Since the activation energy Q is a constant, this spectrum of relaxation times does not change shape with temperature, but only shifts along the τ scale. Thus by obtaining $N(\ell n\ \tau_0)$ and Q we know the spectrum of relaxation times at any given temperature. Substituting the Arrhenius relation Eq. (4) into Eqs. (1), (8), and (9) we obtain for the internal friction as a function of temperature

$$\tan \phi(T) = \frac{\delta J \int_{-\infty}^{\infty} N(\ell n\ \tau_0)\ \frac{\omega \tau_0 \exp(Q/kT)}{1 + \omega^2 \tau_0^2 \exp(2Q/kT)}\ d\ \ell n\ \tau_0}{J_u + \delta J \int_{-\infty}^{\infty} N(\ell n\ \tau_0)\ \frac{1}{1 + \omega^2 \tau_0^2 \exp(2Q/kT)}\ d\ \ell n\ \tau_0} \qquad (15)$$

Eq. (15) has a Fredholm type of integral equation in both the numerator and the denominator. To obtain the approximate solution for $N(\ell n\ \tau_0)$ for n bins we follow the same procedure for taking a sum approximation as was used before but making use of the magnitude of the relaxation as $\delta J_i = \delta J\ A_i$ and $\Sigma\ \delta J_i = \delta J$ to obtain

$$\tan\phi(T) \cong \frac{\sum_{i=1}^{n} \delta J_i \frac{\omega\tau_{o_i} \exp(Q/kT)}{1+\omega^2\tau_{o_i}^2 \exp(2Q/kT)}}{J_u + \sum_{i=1}^{n} \delta J_i \frac{1}{1+\omega^2\tau_{o_i}^2 \exp(2Q/kT)}} \qquad (16)$$

Here τ_{o_i} is the value of the pre-exponential factor in the i^{th} bin and the histogram is for a spectrum of these factors.

Eq. (16) may then be used with the DSA method if we choose values for the number of bins n and the spectral limits τ_{o_s} and τ_{o_f} and supply the values for k and ω. For Eq. (16), however, the analysis is different because in addition to the relaxation magnitudes δJ_i we also use the nonlinear regression analysis to obtain the values for the activation energy Q and the unrelaxed compliance J_u. Thus we must set the number of bins with the constraint $n \leq m - 2$. The conversion to obtain $N(\ell n\ \tau_i)$ the spectral amplitude of the i^{th} bin is then obtained using Eq. (12a) and $A_i = \delta J_i / \delta J$. Finally the relaxation strength Δ can then be compared with experiment using $\Delta = \Sigma\ \delta J_i / J_u$.

Distribution of Q Only

This distribution assumes a constant τ_o and an activation energy distribution function N(Q). Knowing N(Q) and τ_o one can use the Arrhenius relation to convert to $N(\ell n\ \tau)$ at any given temperature. This result can then be compared to a comparable spectrum obtained by the method just described. Again, substituting the Arrhenius relation we obtain for the internal friction an expression analagous to Eq. (15)

$$\tan\phi(T) = \frac{\delta J \int_{-\infty}^{\infty} N(Q) \frac{\omega\tau_o \exp(Q/kT)}{1+\omega^2\tau_o^2 \exp(2Q/kT)}\, d\ \ell n\, Q}{J_u + \delta J \int_{-\infty}^{\infty} N(Q) \frac{1}{1+\omega^2\tau_o^2 \exp(2Q/kT)}\, d\ \ell n\, Q} \qquad (17)$$

To obtain Eq. (17) in a form appropriate for the DSA we again take the sum approximation for n bins to obtain

$$\tan\phi(T) \cong \frac{\sum_{i=1}^{n} \delta J_i \frac{\omega\tau_o \exp(Q_i/kT)}{1+\omega^2\tau_o^2 \exp(2Q_i/kT)}}{J_u + \sum_{i=1}^{n} \delta J_i \frac{1}{1+\omega^2\tau_o^2 \exp(2Q_i/kT)}} \qquad (18)$$

where Q_i is the value of the activation energy in the i^{th} bin.

To do the DSA for n bins using Eq. (18) we divide the activation energy spectrum up into n equal intervals of width δQ, set the spectral limits for the activation energy spectrum Q_s and Q_f, set the pre iteration values for the spectral density of the activation energy in the i^{th} bin to a starting value Q_o, and input the known values for ω and k. For this case the DSA will give values for the spectral density δJ_i plus values for τ_o and J_u. As with Eq. (16) the magnitude of the relaxation is obtained from $\Sigma\ \delta J_i = \delta J$ while the spectral amplitude of the i^{th} bin is again obtained from Eq. (12a).

It should be noted that the success of the DSA method using Eq. (15) or (17) is not expected to be sensitive to the kernel of the integral equation in the denominator because the second term in the denominator is expected to be small with respect to unity. Also, for

experimental situations in which the variation of the frequency ω with temperature can not be ignored by assuming a constant frequency, the experimental values of $\omega(T)$ can be substituted into either Eq. (16) or (18).

Conclusions

(1) The one most important conclusion of this paper is that a method has been developed and validated for directly analyzing internal friction and anelastic creep results to obtain a good approximation of the spectrum of relaxation times controlling the kinetics of the anelastic response.

(2) This method, referred to as Direct Spectrum Analysis, has been demonstrated to provide approximations of known input spectra which replicate the position, amplitude, width, and shape of an original input spectrum. The approximations are typically accurate to better than 10% for input spectra consisting of (a) single lognormal and single box distributions and (b) multiple lognormal (up to four peaks) and box distributions (two peaks).

(3) Limits to the capability of the method are due to difficulties in resolving fine structure in the spectra such as the corners of the box distribution or the sharp peak of a very narrow (nearly discrete) spectrum.

(4) Random experimental error in the data tends to limit resolution; however, the method satisfactorily approximates spectra for internal friction data having fractional error with standard deviation $\sigma = 0.01$ and for normalized anelastic creep data having absolute error with standard deviation $\sigma = 0.05$.

(5) The method has been shown in all of the many cases considered to give correct approximations, i.e., it does not converge on approximate solutions which are not close to the known input spectrum.

Acknowledgments

It is a pleasure to acknowledge helpful discussions on development of the DSA method with J. T. Stanley of Arizona State University and T. Manteuffel of the Computing Division of the Los Alamos National Laboratory. Appreciation is also expressed to J. T. Stanley for his critical review of the manuscript.

References

1. A. S. Nowick and B. S. Berry, *Anelastic Relaxation in Crystalline Solids*, Academic Press, New York, 1972.

2. J. R. Cost, "Nonlinear Regression Least-Squares Method for Determining Relaxation Time Spectra for Processes with First-Order Kinetics," J. Appl. Phys., 54 (5) (1983) pp. 2137-2146.

3. J. R. Cost, "A Direct Spectrum Analysis Method for Obtaining the Relaxation Time Spectrum from Relaxation Response Data: Amorphous Metals," pp. 191-199 in *Amorphous Materials: Modeling of Structure and Properties*, V. Vitek, ed.; AIME, New York, 1983.

4. J. R. Cost, "On the Existence of Interstitial Clustering of Oxygen in Nb-O Solid Solutions." Acta, Met., in press.

5. M. R. Osborne, in *Numerical Methods for Nonlinear Optimization*, F. A. Lootsma, ed.; Academic Press, New York, 1972.